Dendrimer-Assisted Self-Assembled Monolayer of Iron Nanoparticles for Vertical Array Carbon Nanotube Growth

Noe T. Alvarez,[†,‡] Alvin Orbaek,[†,‡] Andrew R. Barron,[†,‡,§] James M. Tour,[†,‡,§] and Robert H. Hauge*[,†,‡]

Department of Chemistry, The Richard E. Smalley Institute for Nanoscale Science and Technology, and Department of Mechanical Engineering and Materials Science, Rice University, Houston, Texas 77005

ABSTRACT Self-assembled monolayers (SAMs) of iron oxide nanoparticles have been prepared using carboxylic-acid-terminated dendrimers. The iron-containing SAM was used as the catalyst for growth of vertical arrays of carbon nanotubes (CNTs). This approach has the potential for producing diameter controlled CNTs from premade catalyst nanoparticles as well as large scale production of CNTs by chemical vapor deposition.

KEYWORDS: nanotubes • catalyst • nanoparticles • monolayer • self-assembly

Since their discovery, carbon nanotubes (CNTs) have become a material central to the field of nanotechnology. Their physical properties (1, 2) have the potential to impact a wide range of applications, including the development of field emitters (3, 4), capacitors (5, 6), field-effect transistors (7), applications in radio-receptor devices (8, 9), energy storage (10), and fiber and coating composites (11, 12), among others. Some of these applications demand large-scale synthesis of CNTs; however, CNT mass production is still an inefficient and expensive process. Of the many CNT synthesis methods, those that grow vertical array (VA)-CNTs have several advantages, such as alignment, control over the CNT length, and reduced catalyst content. Unfortunately, the known processes for the creation of the catalysts for VA-CNT growth require the use of vacuum deposition conditions, such as electron beam evaporation of iron. Such methods are not as conducive to scale-up as an all liquid phase process. In such an approach, a suitable pro-catalyst would be synthesized by wet chemistry techniques that allow for control over the particle diameter and composition. These particles would then be assembled into a two-dimensional monolayer on the catalyst support surface for VA-CNT growth. Spin coating-enabled deposition of thin layers of catalyst that support VA-CNT growth has been reported (13, 14), however, our studies have shown that control of monolayer formation over large areas using spin coating is not straightforward. Here we report that VA-CNT growth may be accomplished from iron oxide nanoparticle pro-catalysts that are deposited as a self-assembled monolayer (SAM) on alumina substrates that have been shown to be a key component for successful VA-CNTs growth (15−17). The particle assembly takes place through $-CO_2H$-terminated dendrimers binding to the substrates as well as the catalyst nanoparticle.

It has been shown that $-CO_2H$ terminated metal oxide nanoparticles may be used as catalyst precursors for the arrays and surface growth of CNTs (18−20); in addition, the exchange of iron oxide-based nanoparticle $-CO_2H$ ligands readily occurs (21). Thus, with a $-CO_2H$ terminated surface on the alumina substrate the nanoparticle pro-catalysts are expected to form a SAM. In separate studies we have shown that the most efficient ligand for binding to an alumina surface is the CO_2H group (22−25). Based on the forgoing criteria a suitable coupling ligand would be a molecule with many terminal $-CO_2H$ groups such as a $-CO_2H$-terminated polyamidoamine dendrimer (PAMAM-CO_2H). When PAMAM-CO_2H interacts with the alumina surface, it does through multiple $-CO_2H$ moieties (23, 25); however, the large number of terminal $-CO_2H$ groups ($n = 128$) and the spherical shape of the dendrimer particle will mean that some number of $-CO_2H$ groups will not be bound to the alumina surface. These free $-CO_2H$ groups can undergo ligand exchange with the $-CO_2H$ from the oleic acid on the nanoparticle until the dendrimer surface is saturated with pro-catalyst nanoparticles (Scheme 1). Once nanoparticles cover the dendrimer surface and all the terminal $-CO_2H$ group are occupied, there is no chemical driving force for more particles to form on the surface, producing monolayer coverage. Prior studies (26) have shown that at pH 7 and above, multilayer dendrimers are not formed.

Monolayers of PAMAM-CO_2H ($G = 4.5$; $M_W = 26\,251.86$) were deposited at 60 °C by dipping alumina-coated silicon wafers in a PAMAM-CO_2H/MeOH solution (132 μM). Subsequently, the PAMAM-CO_2H functionalized alumina was ex-

* Corresponding author. E-mail: hauge@rice.edu.
Received for review October 2, 2009 and accepted December 7, 2009
† Department of Chemistry, Rice University.
‡ The Richard E. Smalley Institute for Nanoscale Science and Technology, Rice University.
§ Department of Mechanical Engineering and Materials Science, Rice University.
DOI: 10.1021/am900666w

Scheme 1. Cartoon Illustrating the Dendrimer-Assisted Formation of a SAM of Fe Nanoparticles on Al_2O_3 Substrates That Leads to the Production of a Vertical Array of Carbon Nanotubes

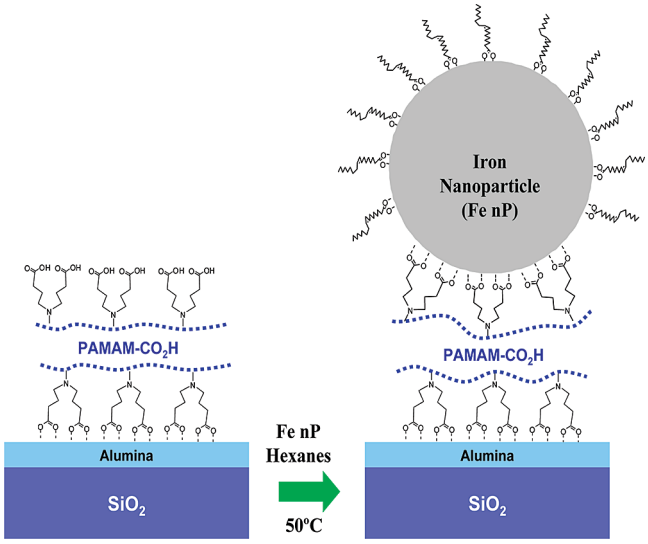

posed to oleic-acid-functionalized iron oxide nanoparticles (4.3 nm mean diameter, 2.0 and 11.5 nm min and maximum diameter, respectively) in hexane in a closed vial at 50 °C for 30 min, followed by a MeOH rinse and wash. After being washed, the substrates were dried with N_2 and calcined at 375 °C under air before being placed in the CNT growth reactor described elsewhere (27, 28). CNT growth was carried out at 750 °C for 15 min using C_2H_2 as the carbon source. H_2 and H_2O were provided in a manner similar to that of the supergrowth technique (28, 29). Prior to growth, atomic hydrogen from a hot tungsten filament was used to reduce the iron oxide nanoparticles for 30 s (27, 28). The AFM image (Figure 1a) of the dendrimer-assisted SAM prior to CNT growth shows a uniform textured surface with individual features consistent with the catalyst particle size. Ellipsometry measurements indicate a dendrimer/pro-catalyst film thickness of 22 nm. Although this is larger than the average diameter of the iron oxide pro-catalyst nanoparticles (4.3 nm, AFM and TEM images in the Supporting Information, Figure S1), it is consistent with monolayer formation given the inclusion of the nanoparticles and the linkage dendrimer (30). Additional evidence for monolayer formation are the XPS measurements; the SAM nanoparticle film gives a Al signal intensity similar to a typical 1 nm evaporated iron catalyst (Figure 1b). Given the special limitations of the SAM film (30) versus the more densely evaporated film, this is reasonable. In fact, the less dense arrangement of the SAM is indicated by a comparison with an evaporated Fe film of comparable depth to the average nanoparticle diameter (i.e., 4 nm). As may be seen from Figure 1b, the 4 nm evaporated film has an Al signal intensity at least four times less than our nanoparticle SAM film. Furthermore, as expected, the Fe signal intensity is less for our nanoparticle SAM film than the evaporated film (see the Supporting Information, Figure S2).

VA-CNTs grown from preformed nanoparticles have been reported in the past; when small-diameter particles were used, larger CNT diameters were observed. This is likely an indication that when the particles were sintered they coalesced to form larger particles, that more than one particle layer was present, and/or that the lateral spatial distribution was nonuniform (18). If there are multiple layers of particles, then it would be expected that sintering and ripening effects would take place and the subsequently larger catalyst particles would then produce larger diameter CNTs than the original or parent catalyst particles (18, 31). Therefore, a monolayer arrangement of particles is considered necessary to achieve reliable correlation between the size of the particle and the diameters of the CNTs produced from the particles. The VA-CNTs grown from SAMs of catalyst nanoparticles produced in this work are similar in length to typical evaporated catalyst samples (Figure 2a). The VA-CNTs are free-standing, cover the entire surface of the substrate and have a height of ~25 μm (Figure 2b and the Supporting Information, Figure S3). This is unlike CNTs grown from catalyst layers, which were produced using spin coating or drop drying, where irregular patches of CNTs were often observed. The VA-CNTs grown from the preformed nanoparticle SAMs have typical diameters of 4−5 nm (Figure 3a and the Supporting Information, Figure S4) and the number

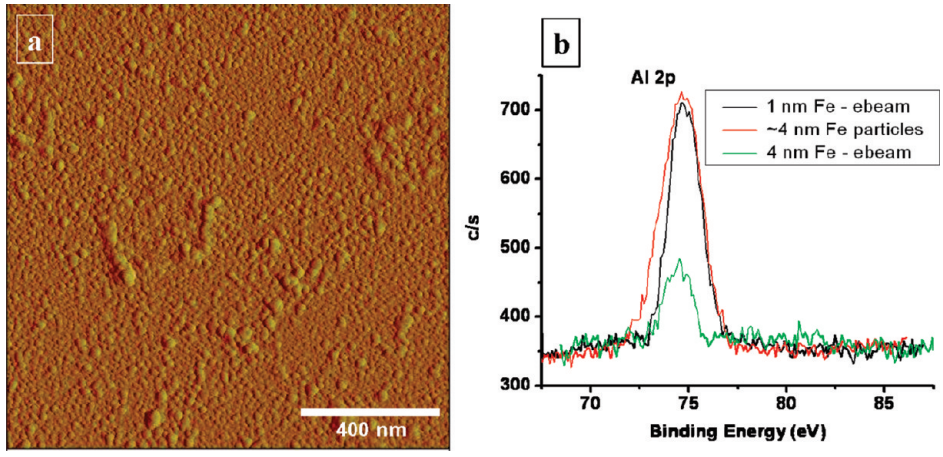

FIGURE 1. (a) AFM image of dendrimer-assisted iron oxide nanoparticle monolayer film and (b) XPS spectra of the Fe nanoparticle monolayer film compared to 1 and 4 nm thick electron beam evaporated Fe catalyst.

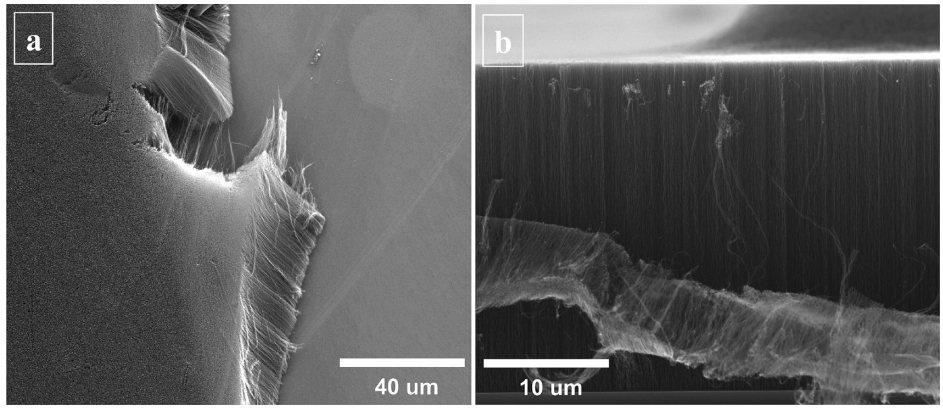

FIGURE 2. SEM images of VA-CNTs grown from dendrimer-assisted iron oxide nanoparticle monolayers: (a) top view and (b) side view of the VA-CNTs.

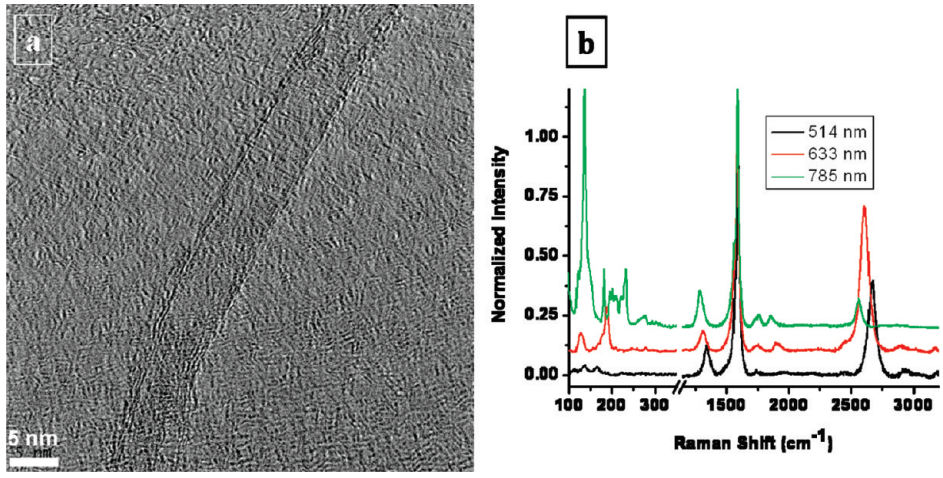

FIGURE 3. (a) TEM images and (b) Raman spectra of VA-CNTs grown from dendrimer-assisted iron oxide nanoparticle monolayer films.

of walls is in the 2−4 range by TEM analysis. VA-CNTs were sonicated in ethanol for 15 min before drying a drop of the CNT dispersion on lacey carbon TEM grid. The Raman spectra taken on solid samples at 514, 633, and 785 nm excitation wavelength show that VA-CNTs are similar to CNTs grown from electron beam evaporated catalyst (Figure 3b). The D/G ratios are low and their length is in the same range.

The technique described herein opens a route to diameter controlled production of VA-CNTs; we think it will be possible to determine the VA-CNT diameter prior to growth based on control of the particle size. This work is in progress. The use of dendrimers in CNT growth has been previously explored, but is limited to assisting in diameter control of the catalyst particles when synthesized in the liquid phase (32−35). In contrast, our use of dendrimers allows for solution-based deposition of a SAM of predetermined size catalyst that allows for successful growth of VA-CNTs.

In summary, we report the preparation of a SAM of a predetermined size of iron oxide nanoparticles on an alumina surface. This self-saturated SAM film provides diameter controlled growth of VA-CNTs.

Experimental Section. Iron oxide nanoparticles were synthesized using a modification of the method by Sun and Zeng (36) where Fe(III) acetylacetonate is used in a condensation reaction using an excess 1,2-hexadecanediol in the presence of oleic acid and olyel amine. The reactants were mixed in solution with benzyl ether as solvent and reflux for 45 min. Then, excess ethanol was added to precipitate the particles and the mixture was centrifuged for 5 min at 4000 rpm, this process was repeated to further remove the organic solvents. The particles were redispersed in hexanes with assistance of additional oleic acid. For the polyamidoamine dendrimer (PAMAM-CO_2H) monolayer self-assembly, PAMAM-CO_2H was diluted in methanol and heated to 60 °C. Alumina coated Si wafer substrate was dipped into the methanol/ PAMAM-CO_2H solution and keep at 60 °C for 30 min. The substrate was removed from solution and dipped into clean methanol and rinsed further with methanol. The substrate was dried with N_2 flow and dipped into the Fe nanoparticle/hexanes solution for 30 min at 50 °C. The substrate was removed and dipped into clean methanol and further rinse with methanol. These substrate with dendrimer/catalyst were placed into the CNT growth reactor at 750 °C for 15 min. The CNT growth protocol uses a 30 s atomic hydrogen reduction and then C_2H_2, H_2O, H_2 were supplied during the growth period, which is described elsewhere (27, 28). All chemicals and solvents were purchased from Sigma Aldrich (Milwaukee, WI) and they were used as purchased without any additional treatment. AFM images were recorded with a NanoScope IIIa, Digital Instruments (Veeco Metrology group, Santa Barbara CA), in tap-

ping mode. SEM images were taken with an environmental SEM (FEI Quanta 400) at 20 KV, XPS spectra was collected with a PHI Quantera SXM (Chanhassen, MN), TEM micrographs were taken with JEOL field emission gun transmission electron microscopy. The Raman spectra was collected with an inVia micro-Raman spectrometer (Renishaw, Gluocestershire, U.K.).

Acknowledgment. We thank Cary Pint, Erik H. Haroz, and Carter Kitrell for helpful discussions; Aldo Frosinini for his assistance with the AFM; and Dr. Angel Marti for his instrumental assistance. This work was supported by the Air Force Laboratories under Contract FA8650-05-D-5807, Air Force Office of Scientific Research, FA9550-09-1-0581, Materials Science and Engineering, Oak Ridge National Laboratory, Department of Energy (Subcontract DE-4000064987), and the Robert A. Welch Foundation.

Supporting Information Available: AFM and TEM images of the iron oxide nanoparticles, XPS of iron oxide nanoparticles film, SEM of VA-CNTs, and TEM of the individual CNTs (PDF). This material is available free of charge via the Internet at http://pubs.acs.org.

REFERENCES AND NOTES

(1) Dresselhaus, M. S.; Dresselhaus, G.; Avouris, P. *Carbon Nanotubes Synthesis, Structure, Properties and Applications*; Springer-Verlag: Berlin, 2001.
(2) Saito, R.; Dresselhaus, G.; Dresselhaus, M. S. *Physical Properties of Carbon Nanotubes*; Imperial College Press: London, 1998.
(3) Rakhi, R. B.; Sethupathi, K.; Ramaprabhu, S. *Carbon* **2008**, *46*, 1656–1663.
(4) Jung, S. M.; Jung, H. Y.; Suh, J. S. *Carbon* **2008**, *46*, 1973–1977.
(5) Kimizuka, O.; Tanaike, O.; Yamashita, J.; Hiraoka, T.; Futaba, D. N.; Hata, K.; Mashida, K.; Suematsu, S.; Tamamitsu, K.; Saeki, S.; Yamada, Y.; Hatori, H. *Carbon* **2008**, *46*, 1999–2001.
(6) Chou, S.; Wang, J.; Chew, S.; Liu, H.; Dou, S. *Electrochem. Commun.* **2008**, *10*, 1724–1727.
(7) Javey, A.; Guo, J.; Farmer, D. B.; Wang, Q.; Yenilmez, E.; Gordon, R. G.; Lundstrom, M.; Dai, H. *Nano Lett.* **2004**, *4*, 1319–1322.
(8) Rutherglen, C.; Burke, P. *Nano Lett.* **2007**, *7*, 3296–3299.
(9) Jensen, K.; Weldon, J.; Garcia, H.; Zettl, A. *Nano Lett.* **2007**, *7*, 3508–3511.
(10) Pushparaj, V. L.; Shaijumon, M. M.; Kumar, A.; Murugesan, S.; Ci, L.; Vajtai, R.; Linhardt, R. J.; Nalamasu, O.; Ajayan, P. M. *Proc. Natl. Acad. Sci. U.S.A.* **2007**, *104*, 13574–13577.
(11) Thostenson, E. T.; Chou, T. W. *J. Phys. D: Appl. Phys.* **2002**, *35*, L77–L80.
(12) Sureeyatanapas, P.; Young, R. J. *Comput. Sci. Technol.* **2009**, *69*, 1547–1552.
(13) Nishino, H.; Yasuda, S.; Namai, T.; Futaba, D. N.; Yamada, T.; Yumura, M.; Iijima, S.; Hata, K. *J. Phys. Chem. C* **2007**, *111*, 17961–17965.
(14) Gunjishima, I.; Inoue, T.; Yamamuro, S.; Sumiyama, K.; Okamoto, A. *Jpn. J. Appl. Phys.* **2007**, *46*, 3700–3703.
(15) Ciambelli, P.; Sannino, D.; Sarno, M.; Leone, C.; Lafont, U. *Diamond Relat. Mater.* **2007**, *16*, 1144–1149.
(16) Aghababazadeh, R.; Mirhabibi, A. R.; Ghanbari, H.; Chizari, K.; Brydson, R. M.; Brown, A. P. *J. Phys.: Conf. Series* **2006**, *26*, 135–138.
(17) Hongo, H.; Nihey, F.; Ichihashi, T.; Ochiai, Y.; Yudasaka, M.; Iijima, S. *Chem. Phys. Lett.* **2003**, *380*, 158–164.
(18) Nishino, H.; Yasuda, S.; Namai, T.; Futaba, D. N.; Yamada, T.; Yumura, M.; Iijima, S.; Hata, K. *J. Phys. Chem. C* **2007**, *111*, 17961–17965.
(19) Crouse, C. A.; Maruyama, B.; R., C. J.; Back, T.; Barron, A. R. *J. Am. Chem. Soc.* **2008**, *130*, 7946–7954.
(20) Cheung, C. L.; Kurtz, A.; Park, H.; Lieber, C. M. *J. Phys. Chem. B* **2002**, *106*, 2429–2433.
(21) Ogrin, D.; Barron, A. R. *J. Cluster Sci.* **2007**, *18*, 7946–7954.
(22) Vogelson, C. T.; Keys, A.; Edwards, C. L.; Barron, A. R. *J. Mater. Chem.* **2003**, *13*, 291–296.
(23) Bethley, C. E.; Aitken, C. L.; Harlan, C. J.; Koide, Y.; Bott, S. G.; Barron, A. R. *Organometallics* **1997**, *16*, 329–341.
(24) Landry, C. C.; Pappe, N.; Mason, M. R.; Apblett, A. W.; Tyler, A. N.; Macinnes, A. N.; Barron, A. R. *J. Mater. Chem.* **1995**, *5*, 331–341.
(25) Koide, Y.; Barron, A. R. *Organomet.* **1995**, *14*, 4026–4029.
(26) Tomita, S.; Sato, K.; Anzai, J. *J. Colloid Interface Sci.* **2008**, *326*, 35–40.
(27) Xu, Y.; Flor, E.; Kim, M. J.; Hamadani, B.; Schmidt, H.; Smalley, R. E.; Hauge, R. H. *J. Am. Chem. Soc.* **2006**, *128*, 6560–6561.
(28) Pint, C. L.; Nicholas, N.; Pheasant, S. T.; Duque, J. G.; Parra-Vasquez, A. N. G.; Eres, G.; Pasquali, M.; Hauge, R. H. *J. Phys. Chem. C* **2008**, *112*, 14041–14051.
(29) Hata, K.; Futaba, D. N.; Mizuno, K.; Namai, T.; Yumura, M.; Iijima, I. *Science* **2004**, *306*, 1362–1364.
(30) Colorado, J. R.; Crouse, C. A.; Zeigler, C. N.; Barron, A. R. *Langmuir* **2008**, *24*, 8912–8917.
(31) Amama, P. B.; Pint, C. L.; McJilton, L.; Kim, S. M.; Stach, E. A.; Murray, T. M.; Hauge, R. H.; Maruyama, B. *Nano Lett.* **2009**, *9*, 44–49.
(32) Choi, H. C.; Kim, W.; Wang, D.; Dai, H. *J. Phys. Chem. B* **2002**, *106*, 12361–12365.
(33) Amama, P. B.; Maschmann, M. R.; Fisher, T. S.; Sands, T. D. *J. Phys. Chem. B* **2006**, *111*, 10636–10644.
(34) Geng, J.; Li, H.; Zhou, D.; Huck, W. T. S.; Johnson, B. F. G. *Polyhedron* **2006**, *25*, 585–590.
(35) Amama, P. B.; Cola, B. A.; Sands, T. D.; Xu, X.; Fisher, T. S. *Nanotechnology* **2007**, *18*, 1–4.
(36) Sun, S.; Zeng, H. *J. Am. Chem. Soc.* **2002**, *124*, 8204–8205.

AM900666W